PROCEEDINGS OF SPIE

SPIEDigitalLibrary.org/conference-proceedings-of-spie

# FEM simulation for artificial generation of SEM pictures

Duy Duc Nguyen, Jean-Herve Tortai, Patrick Schiavone

Duy Duc Nguyen, Jean-Herve Tortai, Patrick Schiavone, "FEM simulation for artificial generation of SEM pictures," Proc. SPIE 10959, Metrology, Inspection, and Process Control for Microlithography XXXIII, 1095918 (26 March 2019); doi: 10.1117/12.2515181

Event: SPIE Advanced Lithography, 2019, San Jose, California, United States

# FEM simulation for artificial generation of SEM pictures

Duy Duc Nguyen[a,b], Jean-Herve Tortai[a], and Patrick Schiavone[b]

[a]Univ. Grenoble Alpes, CNRS, CEA/LETI Minatec, LTM, F-38054, Grenoble Cedex 9, France
[b]Aselta Nanographics, MINATEC-BHT, 7 Parvis Louis Nel 38040, Grenoble Cedex 9, France

## ABSTRACT

Nowadays, the accuracy of the metrology is becoming more and more a critical issue for microelectronic manufacturing as new technology nodes necessitate more and more rigorous process control. Scanning Electron Microscope (SEM) is the equipment most typically used to measure pattern dimensions. The aim of this study is to model and simulate a synthetic SEM image. This is fulfilled by taking into account the physical phenomena that take place in the sample during the scanning of the electron beam. The considered phenomena are the kinetics of the drift and the diffusion of the charges during the scanning and the secondary electrons emission from the sample into the vacuum. A system of Partial Differential Equations (PDEs) is obtained which defines a system that will be solved using the Finite Element Method. The escaping of the secondary electrons is modeled by applying a Robin boundary condition on the top surface of the sample. By computing the secondary electron emission that originates from the sample during the beam scan, a synthetic SEM image is created.

**Keywords:** Ebeam lithography, Finite Element, FEM, FEniCS, secondary electron emission, synthetic SEM image

## 1. INTRODUCTION

Process control in microelectronics consists in measuring metrics experimentally and to compare these values to the targeted ones. If a too large deviation is observed, the ongoing process is reworked or, if not possible, the product is recycled. The most common technique used for dimensional metrology is top-view Scanning Electron Microscopy due to its reasonable throughput and to its numerous automatic pattern detection and automatic dimension measurement toolbox.

SEM consists in scanning the sample with a narrow focused electron beam that is accelerated at a given energy and to detect the electrons that are "emitted" by the sample during the scanning. By synchronizing the beam position with the detected signal, an image is recorded. Physics that occurs during the scanning of the sample involve interaction of electrons with matter,[3] diffusion of charges in excess, charge migration and recombination of the charges.[7] Electrons matter interactions can be simulated using a Monte Carlo approach[2,3,8] or it can be approximated using a compact model that uses a Point Spread function.[1] Electron matter interactions are processes that can be considered as static while diffusion and recombination are dynamic. The purpose of this work is to model these dynamic processes using FEniCS, a solver that implements the Finite Element Method. Previously published paper pointed out that charge diffusion and migration is strongly depends of the material as expected.[5] In order to generate an artificial SEM image, emitted electrons must be taken into account. It was demonstrated that emission yield of electron from the sample is mathematically formulated by a Robin boundary condition at the specimen's surface.[7]

## 2. DRIFT-DIFFUSION MODEL

The drift diffusion model computed in this study defines a system of three Partial Differential Equations (PDEs) that takes into account the dynamic variation of the electron density, hole density and the induced electrical field that appears when an excess of positive or negative charges exists. Electron and hole densities will tend to equilibrate with time but the SEM beam generates source terms that set the system in a non-equilibrium

Further author information: (Send correspondence to Duy Duc Nguyen) E-mail: duy-duc.nguyen@aselta.com, Telephone: +33 (0) 7 52 91 85 16

Metrology, Inspection, and Process Control for Microlithography XXXIII, edited by Vladimir A. Ukraintsev, Ofer Adan, Proc. of SPIE Vol. 10959, 1095918 © 2019 SPIE · CCC code: 0277-786X/19/$18 · doi: 10.1117/12.2515181

state. Thhe following PDE system must be solved for a given domain (specimen body) where specific boundary conditions are applied:

$$\begin{cases} \varepsilon_0 \varepsilon \nabla \cdot \boldsymbol{E} = q_e\left(p - n\right) & \text{in} \quad \Omega \times (0, t_{end}] \\ \dfrac{\partial n}{\partial t} = \nabla \cdot \boldsymbol{j}_n + S_n - R & \text{in} \quad \Omega \times (0, t_{end}] \\ \dfrac{\partial p}{\partial t} = -\nabla \cdot \boldsymbol{j}_p + S_p - R & \text{in} \quad \Omega \times (0, t_{end}] \end{cases} \tag{1}$$

$$\text{with } \boldsymbol{j}_n = \mu_n n \boldsymbol{E} + D_n \nabla n \text{ and } \boldsymbol{j}_p = \mu_p p \boldsymbol{E} - D_p \nabla p,$$

where $\Omega$ denotes the specimen body, $\partial\Omega$ denotes the boundary of $\Omega$, $t \in (0, t_{end}]$ denotes time variable and time interval. The hole and electron densities are respectively $p\left(\boldsymbol{x}, t\right)$ and $n\left(\boldsymbol{x}, t\right)$, $D_n$ and $D_p$ are the diffusion coefficients and $\mu_n$ and $\mu_p$ the drift mobilities. Electron and hole currents are respectively $\boldsymbol{j}_n\left(\boldsymbol{x}, t\right)$ and $\boldsymbol{j}_p\left(\boldsymbol{x}, t\right)$. The electric field $\boldsymbol{E} = -\nabla\varphi$, $\varphi\left(\boldsymbol{x}, t\right)$ being the potential, depends on $\varepsilon_0$ the absolute permittivity of the vacuum and on $\varepsilon$ the relative permittivity, $q_e$ being the elementary charge. The electrons and holes source terms $S_n\left(\boldsymbol{x}, t\right)$ and $S_p\left(\boldsymbol{x}, t\right)$ are approximated thanks to a 3D Gauss function.[1,4] The holes source term $S_p$ is assumed to be a small fraction of $S_n$.

$$S_n(n,p) = \frac{I_0}{q_e (2\pi)^{3/2} \sigma_x \sigma_y \sigma_z} exp\left(-\left(\frac{(x-Bx)^2}{\sigma_x^2} + \frac{(y-By)^2}{\sigma_y^2} + \frac{(z-(Bz-0.3P))^2}{\sigma_z^2}\right)\right), \; S_p(n,p) = 10^{-5} S_n, \tag{2}$$

The electron beam scans the sample with time, $Bx, By, Bz$ being the coordinate of the center of the spot. A shift in the z direction, denoted as $P$, is inputted. This shift corresponds to the maximum penetration depth of the electrons into the material.[6,7] The order of magnitude of $P$ is a few nanometers. The 3D Gauss function is defined with three spreading values, $\sigma_x, \sigma_y, \sigma_z$ that correspond respectively to the width, the length and the depth of the electron interaction volume. This interaction volume is dependent of the material but moreover it depends of the incident electron beam energy. For CD-SEM, electron energies are usually below 10 keV, the spreading ranges are then in the order of few tenth of nanometer. $I_0$ is the current of the electron beam, typical values ranging from tens of picoamperes up to nanoamperes. Plot of all $(Bx, By, Bz)$ can be found in Figure 2. Once electrons are entrapped in the sample due to the incident beam, a rapid recombination appears that tends to compensate for this electron excess so electro-neutrality is maintained shortly. The recombination term, denoted by $R\left(\boldsymbol{x}, t\right)$, follows the Shockley-Read-Hall model formulated as

$$R(n,p) = \frac{np - n_i^2}{\tau_p(n+n_i) + \tau_n(p+p_i)} \tag{3}$$

where $n_i$ and $p_i$ are the intrinsic carrier concentration, $\tau_n$ and $\tau_p$ the electron and hole average lifetimes.

In order to model the electron emission at the sample surface $\Gamma_R$, a Robin boundary condition is applied. This boundary condition will account for the surface recombination velocity $v_n$.[7]

$$\boldsymbol{j_n} \cdot \boldsymbol{\eta} = v_n(n - n_i) \tag{4}$$

$\boldsymbol{\eta}$ is the outward normal vector at the sample surface. On $\Gamma_R$ the electrons inside the specimen are allowed to pass through it into the surrounding environment whenever the electron concentration is higher than $n_i$. Meanwhile the holes can not move through $\Gamma_R$. The detector, synchronized with the current position of the beam, collects the secondary electron emission from all over the top surface. This is represented by the following equation

$$SEE := \int_{t_{spot}} \int_{\Gamma_R} \boldsymbol{j_n} \cdot \boldsymbol{\eta} \, \mathrm{d}s\mathrm{d}t. \tag{5}$$

where $t_{spot}$ is irradiation time at a spot. The emitted electrons are afterwards collected (on the whole sample surface) and synchronized with the beam position in order to attribute a value to the considered pixel of the synthetic image. We assume that SEM detectors have a signal to noise sensitivity that is proportional to the square root of the electron dose that is deposited by the incident beam of the SEM as reported in [ref]. Each value attributed to each pixel of the artificial SEM image are then proportional to the square root of the simulated SEE number.

In order to set properly the system, other boundary conditions are needed. Those boundary conditions are set at the "edge" of the domain defined by $\Gamma_D$. It is assumed that the potential is null and the carrier densities equal to intrinsic densities at $\Gamma_D$. The mathematical expression of those conditions are Dirichlet boundary conditions:

$$\varphi = 0,\ p = n = n_i \text{ on } \Gamma_D \text{ and } \boldsymbol{j_p} \cdot \boldsymbol{\eta} = 0 \text{ on } \Gamma_R, \tag{6}$$

For dynamic PDE solving, initial conditions shall also be defined. The initial conditions we assumed on $\varphi$, $n$ and $p$ are set as:

$$\varphi(\mathbf{x}, 0) = 0,\ n(\mathbf{x}, 0) = p(\mathbf{x}, 0) = n_i. \tag{7}$$

Once the PDE system is correctly defined, the system can be solved using the Finite Element Method (FEM).

## 3. SIMULATION STRATEGY

FEM is a numerical method for solving PDE systems. The typical implementation consists in transforming the PDE system in a single integral formula named the weak form, that must be minimized during the simulation. The transformation of the PDE system into this weak form(1) is obtained by multiplying each equation of the PDE system with a proper test function and then by integrating by parts at the term which has the highest order in derivative. Then the weak form is defined as the sum of all of these expressions, giving a residue (res) that must be minimized to zero:

$$\begin{aligned} res := \varepsilon_0 \varepsilon \int_\Omega \nabla\varphi \cdot \nabla\overline{\varphi}\ \mathrm{d}x - q_e \int_\Omega (p - n)\,\overline{\varphi}\ \mathrm{d}x + \int_\Omega \frac{\partial n}{\partial t}\overline{n}\ \mathrm{d}x + \int_\Omega \boldsymbol{j}_n \cdot \nabla\overline{n}\ \mathrm{d}x + \int_{\Gamma_R} \boldsymbol{j}_n \cdot \boldsymbol{\eta}\overline{n}\ \mathrm{d}s \\ - \int_\Omega (S_n - R)\,\overline{n}\ \mathrm{d}x + \int_\Omega \frac{\partial p}{\partial t}\overline{p}\ \mathrm{d}x - \int_\Omega \boldsymbol{j}_p \cdot \nabla\overline{p}\ \mathrm{d}x + \int_\Omega (S_p - R)\overline{p}\ \mathrm{d}x = 0, \end{aligned} \tag{8}$$

where $\overline{\varphi}, \overline{n}, \overline{p}$ are the test functions and they are taken arbitrarily from an appropriate functional space containing functions that vanish on $\Gamma_D$.

In this work, the total domain is a rectangular substrate of $300 \times 300 \times 100nm^3$ of size. On the top of the substrate, a trapezoid pattern is defined. Its size is set by $60 \times 60 \times 50nm^3$, and a slope of 80°. One must notice such sharp edges do not exists in real pattern where all edges are rounded. Nevertheless, for sake of simplicity, rounded corner are not considered yet. The boundaries of the pattern are $\Gamma_D$ at the bottom (junction surface with the substrate) and $\Gamma_R$ at the lateral surfaces and at the top surface. The electrons escaping through $\Gamma_R$ are taken into account in equation 4.

Two different materials will be considered, Silicon (Si) that is a semiconductor (fast charge diffusion and migration coefficient) and Silicon Dioxide ($SiO_2$) which is a dielectric where charge diffusion and migration are slow.

Once the geometry is set and the materials chosen, a mesh must be generated to solve the system by the Finite Element Method. Using a uniform mesh with a small size would result in two many voxels (3D pixels) therefore tremendously long computation time. Consequently, designing an adaptive mesh is mandatory. The designed adaptive mesh in this study is dense in the vicinity of the scanning area and in the electron spreading volume but is relaxed outside of the scanning area Figures 2, 1.

The scanning area is 50 nm larger than the pattern dimension and is centered at the pattern position. The beam step size during the scanning is set at 10nm, On purpose, the scanning area is set smaller than the total domain size in order to avoid simulation errors close to the domain boundaries.

The incident beam $S_n$ fully scans the specimen starting from the left to the right and from the top to the bottom. It is defined to stay $5\mu s$ at each spot . The electron spreading into the material (2) at each beam position is assumed to be a symmetrical 3D PSF (i.e. $\sigma_x = \sigma_y = \sigma_z = P$) whose dimensions are considered to be proportional with the material density. For Si it is set equal to $10nm$ and to $8.7nm$ for $SiO_2$.

In order to minimize the residue for every time, it was chosen to use a backward Euler scheme for each time step $5\mu s$. At each time step, we compute SEE using equation (5) and store it together with the beam position $(Bx, By)$ (see Figures 4, 7). This data is also used for interpolation in order to extract value on a horizontal line or a vertical line, Figures 4, 7. It takes 12-24 hours for a simulation depending on the mesh size

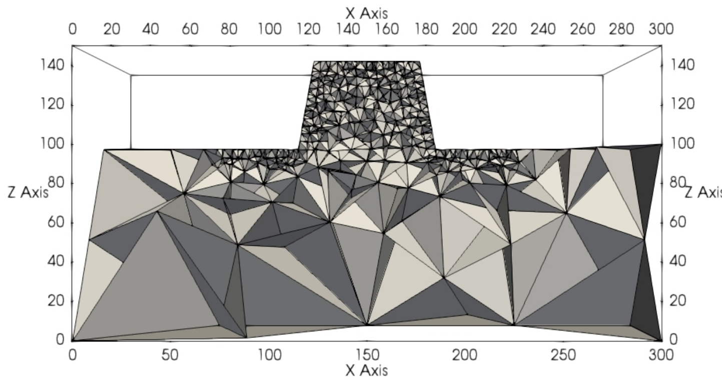


Figure 1: The mesh is set to be dense when it is close to the top surface and within the scanning area and to be coarse in the remaining area.

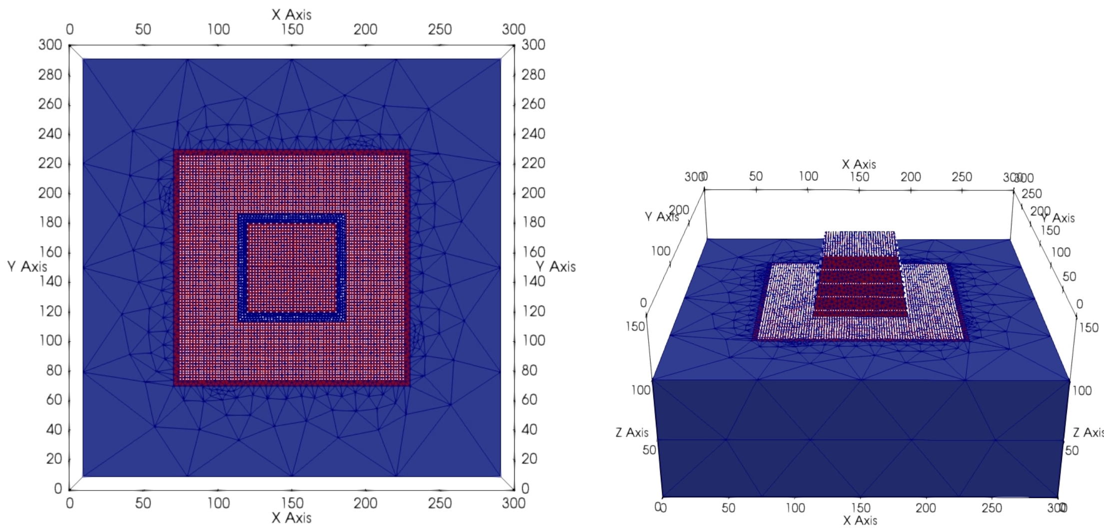


Figure 2: Plot of all beam spots (white dots) $(Bx, By, Bz)$. The surface in red is scanning area where dense mesh is set, the remain surface in blue is set with coast mesh. Only the scanning area will be shown in SEM image.

## 4. SIMULATION RESULTS

We present here two simulations dedicated to the cases where both substrate and pattern are made from Si and $SiO_2$ respectively. In both cases, we conclude some general facts.

### 4.1 SEM simulation in Si sample

For both SEM images shown in Figure 4 and 7 the edges are darker than other parts instead of brighter compared to image obtained from real experiments. This error is most probably due to the SEE formula (5) that is based on the outward normal vector $\boldsymbol{\eta}$ which is not well defined at the corner of the pattern. In a future work, we will replace the sharp corners by rounded ones.

Figure 3 shows how electron density is spreading in the Silicon for three spot positions. At the very beginning (Figure 3(a)), electron density is high only in the vicinity of the spot due to the fast diffusion and migration of the charges in Silicon. When the spot is located at the center of the pattern (Figure 3(b)), electrons are slightly entrapped in the pattern due to the pattern boundaries that act as a diffusion and migration barrier. Finally, at the very end of the scan (Figure 3(c)), a similar electron spreading than for the initial beam position is observed. This proves that the rapid diffusion and migration of the charges prevent any charging effect due to the previously scanned surface. We can observe here that the FEM modeling is consistent with what is expected when considering the charging of semiconductor materials.

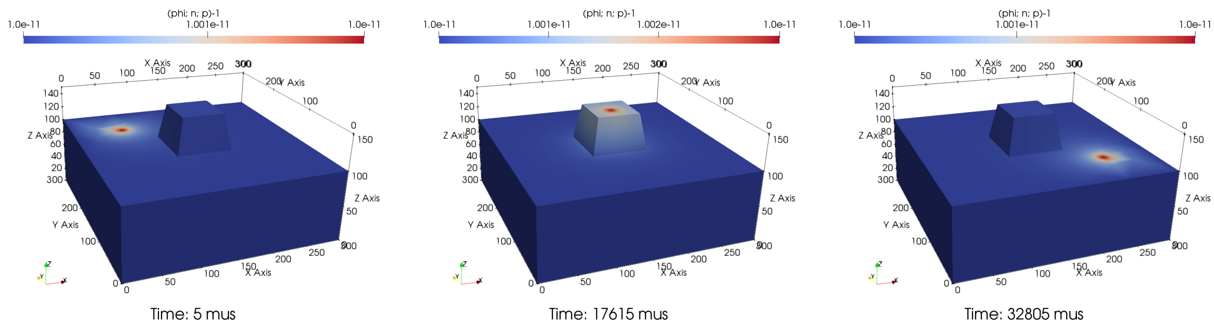


(a) the beginning (b) the middle (c) the end

Figure 3: The concentration of electron in Si-Si Simulation at the beginning, at the middle and at the end of the scanning process.

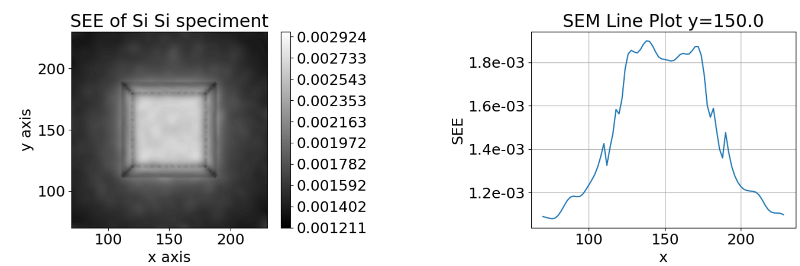


(a) SEM image (b) Y-line at $y = 150$ [nm]

Figure 4: Synthetic SEM image of Si-Si simulation and SEM signal measurements.

## 4.2 SEM simulation in SiO2 sample

Figure 5 shows the spreading of the electron densities in the $SiO_2$ for the same spot positions as in previous section. $SiO_2$ is a dielectric so electron drift and diffusion are very slow compared to Si. Comparing Figure 5(a) with Figure 5(c), the electron density distribution does not look alike. This points out the charging of the sample during the scan. At the end of the scan, the pattern still shines with a high electron density in it. When the spot is located at the center of the pattern for the intermediate time (Figure 5(b) ), electrons are entrapped in the pattern and an asymmetry is clearly observed. The previously scanned areas of the pattern still have a large electron density. These FEM results are consistent with the fact that charging effects more likely occur when scanning a dielectric sample with a SEM.

Figure 6 focuses on the potential at the surface of the SiO2 sample at same three spot positions. It confirms the charging effect of the sample during the scanning. Obviously, it should be taken into account in the future in order to mitigate the SEE efficiency with its value.

The synthetic SEM image 7 obtained with SiO2 shows an anomalous contrast in the upper part compared to the lower part. We did expect that the total SEE at the later spot might be higher than the previous one due to the way of the detector collects electrons. The SEM detector response is modelled by integrating the SEE signal on the whole sample surface during the time the spot stays at a given position. Because of the previously scanned surface, the detector collects electrons that escape the sample surface due to the spot by itself but it also collects electrons that escapes from other previously scanned area where charges are still in excess. SEE emission only stops when the electron concentration reaches the intrinsic electron density, i.e $n = n_i$. As for Si patterns, the concentration of electron increases as expected when the pattern is scanned. Again, the pattern boundaries

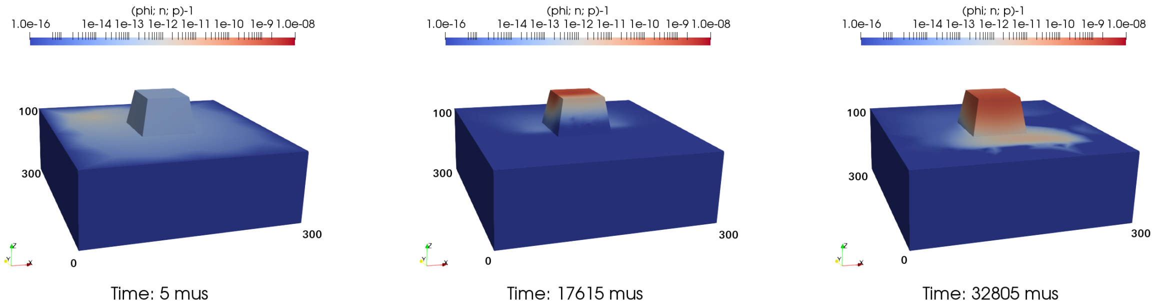


(a) the beginning (b) the middle (c) the end

Figure 5: The concentration of electron in $SiO_2$-$SiO_2$ Simulation at the beginning, at the middle and at the end of the scanning process.

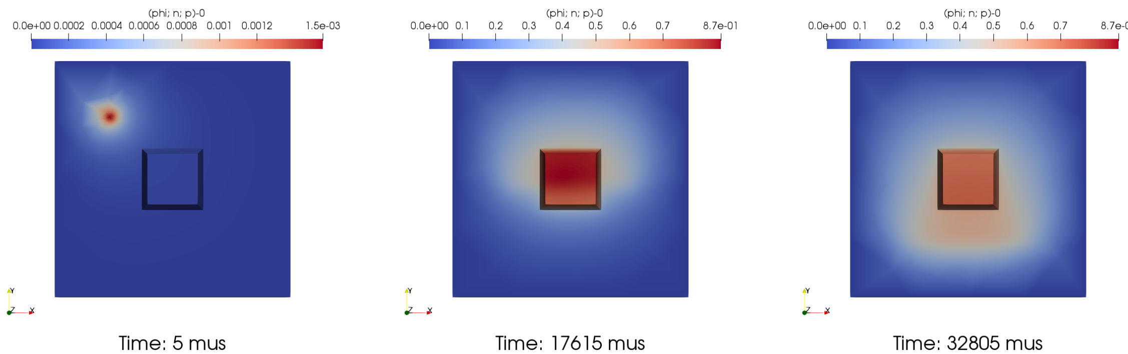


(a) the beginning (b) the middle (c) the end

Figure 6: The concentration of potential in $SiO_2$-$SiO_2$ Simulation at the beginning, at the middle and at the end of the scanning process.

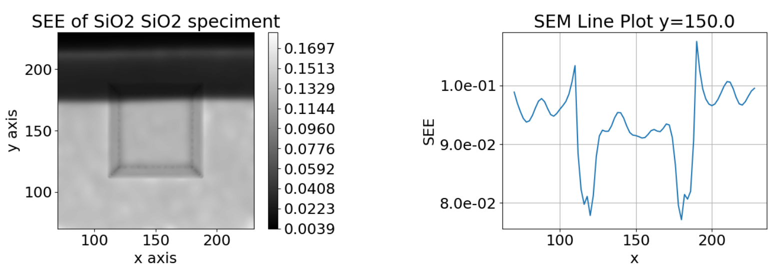


(a) SEM image (b) Y-line at $y = 150$ [nm]

Figure 7: Synthetic SEM image of $SiO_2$-$SiO_2$ simulation and SEM signal measurements.

act as a diffusion and migration barrier so less freedom is allowed to charges to move. Those electrons will slowly diffuse and therefore will continue to contribute to the SEE signal until the end of the scanning process. The SEE signal generated by the pattern is a main contributor for the detector. Looking at the contrast of the the artifact SEM signal in the middle of the pattern, it looks quite similar to the real contrast obtained when a real SEM measures CD of patterns. But the anomalous contrast in the vertical direction points out an imperfect calibration of the model, certainly due to the detector modelling or to the surface potential that impacts on SEE efficiency.

## 5. CONCLUSION AND PERSPECTIVE

It was demonstrated that using the Finite Element Method it is possible to generate synthetic SEM images. The algorithm implemented in this study allows to simulate a full scan of a virtual sample. By solving the PDE system using FEM, it allows to monitor the time variation of the electrons and holes densities and the variation of the electric potential during the scanning. Meanwhile, the Secondary Electron Emission is simulated and synchronized with the beam position. From that, a SEM signal can be computed. The synthetic SEM signal we obtained exhibits similar contrast as real SEM images when a pattern is scanned. However, in the current implementation, we observed that the charging effect in dielectrics is overestimated. To be more realistic, further developments are ongoing in order to take into account the charges that are entrapped, the surface potential that impacts the SEE efficiency and the vacuum model that is not yet considered.

## REFERENCES


1. Benjamin Alles, Eric Cotte, Bernd Simeon, and Timo Wandel. Modeling the work piece charging during e-beam lithography. In *SPIE Advanced Lithography*, pages 69244P–69244P. International Society for Optics and Photonics, 2008.
2. Sergey Babin, Sergey S Borisov, Hiroyuki Ito, Andrei Ivanchikov, and Makoto Suzuki. Simulation of scanning electron microscope images taking into account local and global electromagnetic fields. *Journal of Vacuum Science & Technology B, Nanotechnology and Microelectronics: Materials, Processing, Measurement, and Phenomena*, 28(6):C6C41–C6C47, 2010.
3. Dominique Drouin, Alexandre Réal Couture, Dany Joly, Xavier Tastet, Vincent Aimez, and Raynald Gauvin. Casino v2. 42a fast and easy-to-use modeling tool for scanning electron microscopy and microanalysis users. *Scanning*, 29(3):92–101, 2007.
4. A Maslovskaya and A Pavelchuk. Simulation of dynamic charging processes in ferroelectrics irradiated with sem. 476(1):1–11, 2015.
5. Duy Duc Nguyen, Jean-Herve Tortai, Mohamed Abaidi, and Patrick Schiavone. Fem simulation of charging effect during sem metrology. In *34th European Mask and Lithography Conference*, volume 10775, page 107750P. International Society for Optics and Photonics, 2018.
6. Behrouz Raftari, Neil Budko, and Kees Vuik. A modified and calibrated drift-diffusion-reaction model for time-domain analysis of charging phenomena in electron-beam irradiated insulators. *AIP Advances*, 8(1):015307, 2018.
7. Behrouz Raftari, NV Budko, and C Vuik. Self-consistent drift-diffusion-reaction model for the electron beam interaction with dielectric samples. *Journal of Applied Physics*, 118(20):204101, 2015.
8. John S Villarrubia, AE Vladár, Bin Ming, Regis J Kline, Daniel F Sunday, JS Chawla, and Scott List. Scanning electron microscope measurement of width and shape of 10nm patterned lines using a jmonsel-modeled library. *Ultramicroscopy*, 154:15–28, 2015.